Swansea University
Prifysgol Abertawe

Cronfa
Setting Research Free

Cronfa - Swansea University Open Access Repository

This is an author produced version of a paper published in:
ACS Applied Materials & Interfaces

Cronfa URL for this paper:
http://cronfa.swan.ac.uk/Record/cronfa44667

Paper:
Fuoco, A., Comesaña-Gándara, B., Longo, M., Esposito, E., Monteleone, M., Rose, I., Bezzu, C., Carta, M., McKeown, N. et. al. (2018). Temperature Dependence of Gas Permeation and Diffusion in Triptycene-Based Ultrapermeable Polymers of Intrinsic Microporosity. *ACS Applied Materials & Interfaces, 10*(42), 36475-36482.
http://dx.doi.org/10.1021/acsami.8b13634

This item is brought to you by Swansea University. Any person downloading material is agreeing to abide by the terms of the repository licence. Copies of full text items may be used or reproduced in any format or medium, without prior permission for personal research or study, educational or non-commercial purposes only. The copyright for any work remains with the original author unless otherwise specified. The full-text must not be sold in any format or medium without the formal permission of the copyright holder.

Permission for multiple reproductions should be obtained from the original author.

Authors are personally responsible for adhering to copyright and publisher restrictions when uploading content to the repository.

http://www.swansea.ac.uk/library/researchsupport/ris-support/

Temperature Dependence of Gas Permeation and Diffusion in Triptycene-Based Ultrapermeable Polymers of Intrinsic Microporosity.

Alessio Fuoco[†*], Bibiana Comesaña-Gándara[‡], Mariagiulia. Longo[†], Elisa Esposito[†], Marcello Monteleone[†], Ian Rose[‡], C. Grazia Bezzu[‡∥], Mariolino Carta[⊥], Neil B. McKeown[‡*], Johannes C. Jansen[†]

[†] Institute on Membrane Technology (ITM-CNR), Via P. Bucci 17/C, 87036 Rende (CS), Italy.

[‡] EastChem, School of Chemistry, University of Edinburgh, David Brewster Road, Edinburgh EH9 3FJ, UK

[⊥] Department of Chemistry, College of Science, Grove Building, Singleton Park, Swansea University, Swansea, SA2 8PP, UK

ABSTRACT: A detailed analysis of the basic transport parameters of two triptycene-based polymers of intrinsic microporosity (PIMs), the ultrapermeable PIM-TMN-Trip and the more selective PIM-BTrip, as a function of temperature from 25°C to 55°C, is reported. For both PIMs, high permeability is based on very high diffusion and solubility coefficients. The contribution of these two factors on the overall permeability is affected by the temperature and depends on the penetrant dimensions. Energetic parameters of permeability, diffusivity and solubility are calculated using Arrhenius-van't Hoff equations and compared with those of the archetypal PIM-1 and the ultrapermeable but poorly selective poly(trimethylsilylpropyne) (PTMSP). This considers, for the first time, the role of entropic and energetic selectivities in the diffusion process through highly rigid PIMs. This analysis demonstrates how energetic selectivity dominates the gas transport properties of the highly rigid triptycene PIMs and enhances the strong size-sieving character of these ultrapermeable polymers.

KEYWORDS: Polymer of Intrinsic Microporosity; Ultrapermeability; Gas separation; Temperature dependence; Entropic Selectivity; Energetic Selectivity;

INTRODUCTION

Polymeric membranes are successfully used in a number of industrial processes for gas separation and purification such as N_2 generation, O_2 enrichment of air, hydrogen recovery and natural gas treatment. However, wider implementation is limited by the lack of materials with high permeability, good selectivity and processability.[1,2] Hundreds of new polymers have been investigated to date, but only a few exploited in commercial uses, and these demonstrate low permeability and high selectivity. The lack of permeability means low flux, which for large scale processing, requires infeasible membrane areas. Thus, the use of polymer materials with higher permeability is crucial to providing membrane systems suitable for large scale separations.

In 1991, Robeson quantified the trade-off for the separation of a particular gas mixture between the desired selectivity of a polymer and its permeability.[3] Empirical upper bounds were drawn by Robeson on his now famous double logarithmic plots for a number of commercially interesting gas pairs.[4] On the basis of a theoretical analysis, Freeman confirmed the positions of the upper bounds and suggested that high free volume polymers, with rigid and stiff chains are desirable to prepare better performing membranes, and indicates that the selectivity for diffusion is the key factor to exceed Robeson's upper bounds.[5]

The lack of polymers with high free volume and highly rigid chains was addressed by the invention of Polymers of Intrinsic Microporosity (PIMs), a family of polymers that demonstrated both high permeability and moderate selectivity.[6,7] Recently, the first ultrapermeable PIM (CO_2 permeability > 20000 barrer[8]), namely PIM-TMN-Trip, was reported, providing permselectivity data that filled a previously unpopulated region of the Robeson plot for several gas pairs.[9] In the same paper, the synthesis of PIM-BTrip is also reported but lack of solubility in common casting solvents prevented measurement of its gas permeability data. The superior permselectivity of PIMs, as compared with the unselective ultrapermeable polyacetylenes such as poly(trimethylsilylpropyne) (PTMSP), can be ascribed to the size-sieving character of these very rigid polymers. For instance, whilst PIM-TMN-Trip and PTMSP display similar diffusion coefficients for the fastest gases, He and H_2, bulkier gases are significantly slower in PIM-TMN-Trip as compared to PTMSP. In general, the diffusion coefficient is related to the size of the penetrant gas, the packing density of the polymer chains and their flexibility.[10] For PIMs, and more generally for all semi-rigid polymers, it has been hypothesized that the gas diffusion process is halfway between that in molecular sieves and that in flexible polymers.[11] Koros *et al.* analyzed the gas transport in polymers in terms of energetic and entropic selectivity through measurements at different temperatures, suggesting that in very rigid polymers the gas separation properties are driven by the energetic contribution, while the entropic selectivity is stronger in carbon molecular sieves (CMS).[12–14]

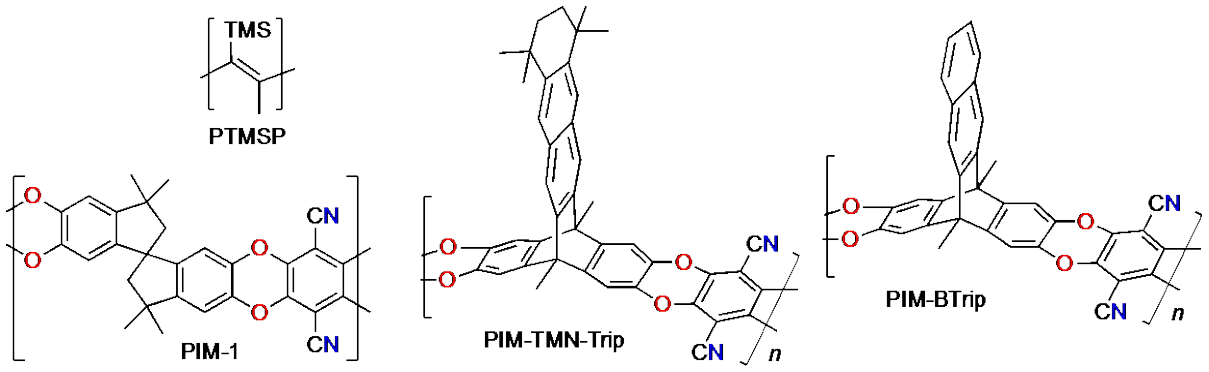

Figure 1. Molecular structures of PTMSP, PIM-1, PIM-TMN-Trip and PIM-BTrip.

This analysis gives important insight into the gas transport in dense polymeric membranes and is fundamental for the development of novel materials and their successful application. Remarkably, in spite of the enormous attention for PIMs in the recent literature, Koros and Zhang pointed out that this analysis is still missing for PIMs.[11] The objective of the present work is therefore to fill this gap by providing an analysis of the permeability, diffusion and solubility coefficients of PIM-TMN-Trip and PIM-BTrip as a function of temperature and to determine activation and sorption energies. Particular attention is paid to the diffusion process of the penetrant and how the size-sieving properties of these PIMs can be expressed in terms of the entropic and energetic selectivity. Such a thorough analysis of the transport properties in PIMs could help to facilitate their use in industrial gas separation processes.

EXPERIMENTAL SECTION

Materials

The PIM-TMN-Trip and PIM-BTrip synthesis are described in a previous paper.[9] Dense self-standing films were prepared by solvent casting from chloroform (PIM-TMN-Trip) and quinoline (PIM-BTrip) and a very slow evaporation of the solvent allowed the formation of mechanically robust and defect-free membranes. It should be noted that PIM-BTrip was previously reported to be insoluble in organic solvents but was subsequently found to be soluble in quinoline which proved to be a suitable casting solvent.[9] Because freshly prepared PIMs membranes are known to undergo physical ageing[15,16], a PIM-TMN-Trip sample aged for 100 days after thermal treatment (heated at 140°C for 4h in vacuum) and a PIM-BTrip sample aged for 250 days were used during the permeation tests to guarantee time independent performance. The precise membrane thickness is 154 µm for the PIM-TMN-Trip and 160 µm for PIM-BTrip.

All gases were supplied by Sapio (Italy) at a minimum purity of 99.9995+%.

Gas adsorption.

The N_2 adsorption isotherms at 77 K were measured using a Quantachrome Autosorb iQ2. The powder samples were degassed for 600 min at 120 °C before the experiment. The adsorption isotherm was used to calculate the pore volume and the pore-size distribution; the Horvath–Kawazoe (HK) model was applied considering the adsorbent geometry as carbon slit pores for all cases.

Gas permeation measurements

Single gas time-lag experiments were performed at four different temperatures (from 25 to 55°C) on a fixed volume / pressure increase instrument (Elektro & Elektronik Service Reuter, Geesthacht, Germany) on circular samples with an effective area of 2.14 cm^2. The feed pressure was 1 bar, and the gases were tested in the order: H_2, He, O_2, N_2, CH_4 and CO_2. A turbo molecular pump guarantees an efficient degassing of the samples, and computer controlled pneumatic valves allow very fast response times. i.e. 0.08 s.[17] Permeability (P) is reported in Barrer (1 Barrer = 10^{-10}·cm^3(STP)·cm·cm^{-2}·s^{-1}·cm Hg^{-1}), and the diffusion coefficient (D) is calculated from the so-called permeation time lag, Θ (s):

$$D = \frac{l^2}{6\Theta} \qquad \text{Eq. 1}$$

where l is the film thickness. The gas solubility coefficient (S) is calculated indirectly assuming the validity of the solution-diffusion model as the ratio of the permeability over the diffusion coefficients:

$$S = \frac{P}{D} \qquad \text{Eq. 2}$$

Considering the instrumental time-lag, any time-lag of about 0.5 s has less than 20% error, which in general results in an underestimation of D. A detailed discussion of the method and calculations can be found in a dedicated work.[17]

RESULTS AND DISCUSSION

Nitrogen (N_2) adsorption isotherms obtained at 77 K for powdered samples of PIM-TMN-Trip and PIM-BTrip (Figure SI 1) confirms the presence of intrinsic microporosity for both polymers by the significant uptake of N_2 at low partial pressures (P/Po < 0.01). These isotherms provide apparent BET surface areas of 1034 m^2 g^{-1} and 911 m^2 g^{-1} for PIM-TMN-Trip and PIM-BTrip, respectively, which are both larger values than for typical PIMs and indicate that

the former has slightly greater intrinsic microporosity than the latter.

Figure 2a-d shows the Robeson plots for four industrially relevant gas pairs: CO_2/CH_4 (biogas treatment), CO_2/N_2 (carbon capture from flue gas), O_2/N_2 (oxygen/nitrogen enrichment of air) and H_2/CH_4 (hydrogen recovery). It is immediately clear that the performances of the aged PIM-TMN-Trip and PIM-BTrip are located well above the 2008 upper bound. The PIM-BTrip surpasses also the proposed 2015 upper bounds for O_2/N_2 and H_2/CH_4, showing excellent gas separation properties. It should be noted that the 2015 upper bounds for O_2/N_2, H_2/N_2 and H_2/CH_4, proposed by Pinnau[18], are based on data obtained from highly rigid triptycene-based PIMs.[19,20] The data of PIM-1[21] and of PTMSP[22] films are reported for comparison. Permeability data for PIM-1 typically fall close to the 2008 upper bounds, which is unsurprising as Robeson used data reported for PIM-1 to reposition the upper bounds.[4] PTMSP gas permeability data is similar to those of PIM-TMN-Trip, but they show low selectivity so that this polymer's data points fall below the original 1991 upper bound. CO_2 gas permeability in the thermally treated 100 day aged PIM-TMN-Trip is similar to that in PTMSP but with much higher selectivity over CH_4 or N_2, while it has similar selectivity to that of a PIM-1 film but much higher permeability. The CO_2 permeability in the 250 days aged PIM-BTrip is still higher than that of PIM-1 and it is significantly more selective. Upon aging, PIM-BTrip shows higher selectivity and similar CO_2 permeability with respect to that of the freshly methanol treated parental polymer PIM-BTrip-TB[23], containing the Tröger's base (TB) 3D contortion site (Figure SI 2). Moreover, the CO_2 permeability in the thermally treated and 100 days aged PIM-TMN-Trip is also higher than that of a freshly methanol treated PIM-TMN-Trip-TB film[9] (Figure SI 2). The comparison of these two polymers of 2D chain structures with the TB-based parental polymers of 3D chain structures, confirms the great importance of the 2D chain structure for reaching high permeability and good selectivity even after long aging or thermal stress. The effect of other variables has been minimized by stabilization of the samples (*i.e.* aging for 100 days after the thermal conditioning of PIM-TMN-Trip, and aging for 250 days for PIM-BTrip), which should be more than sufficient, knowing that the permeability loss of PIM-1 in the first 100 days is larger than that in the subsequent 1000 days. [15]

Figure 3a and b show the variation of gas permeability over the temperature range 25-55 °C for different gases through PIM-TMN-Trip and PIM-BTrip, respectively, showing that the permeation rate in both polymers increases in the order $N_2 < CH_4 < O_2 < He < H_2 < CO_2$, over virtually the entire range of temperature, with exception of He and O_2 which are inverted in PIM-TMN-Trip. The gas permeability coefficients for PIM-TMN-Trip increase with temperature only for bulkier penetrants (N_2 and CH_4), while the permeability of faster penetrants (CO_2 and O_2) decreases, and that of very small penetrants (H_2 and He) is almost constant (Figure 3a).

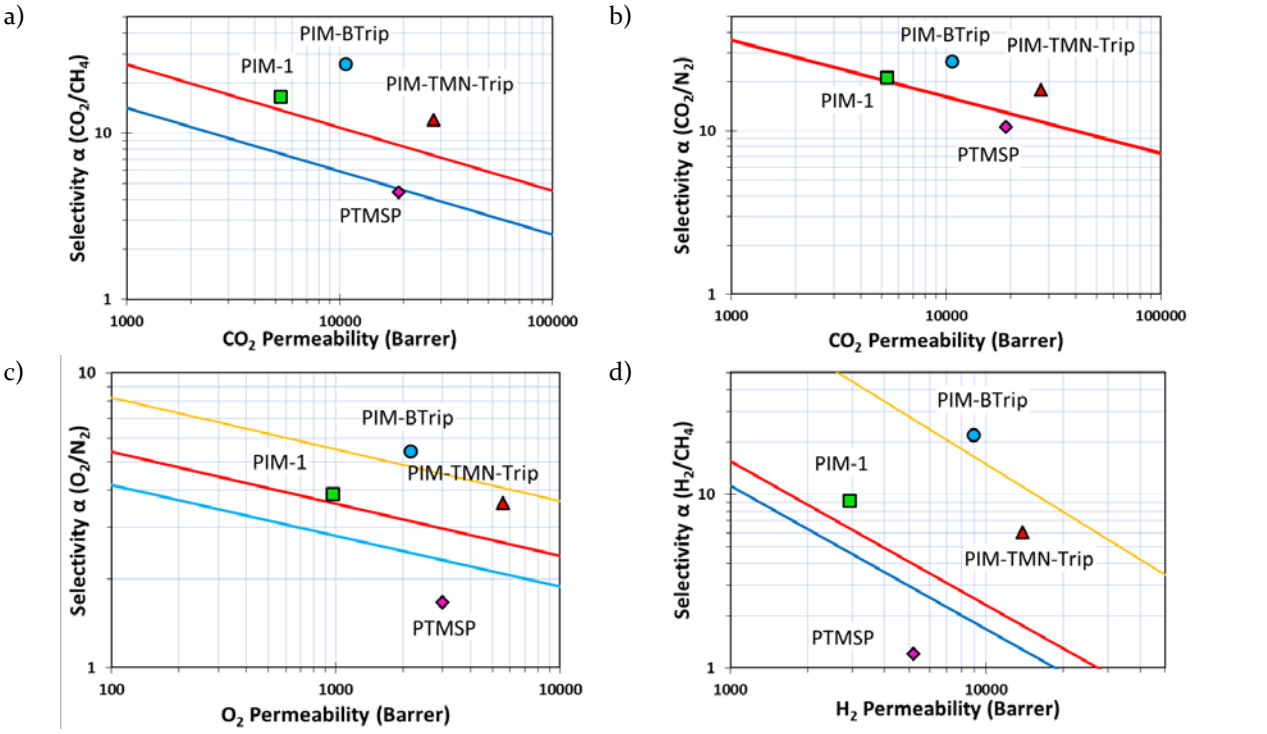

Figure 2. Robeson plots for the a) CO_2/CH_4, (b) CO_2/N_2, (c) O_2/N_2, (d) H_2/CH_4 gas pairs showing the permeability data for PIM-1 (■)[21], PTMSP (◆)[22], PIM-BTrip (●) and PIM-TMN-Trip (▲) at 25°C. Upper bounds are represented in blue (1991), red (2008) yellow (2015).

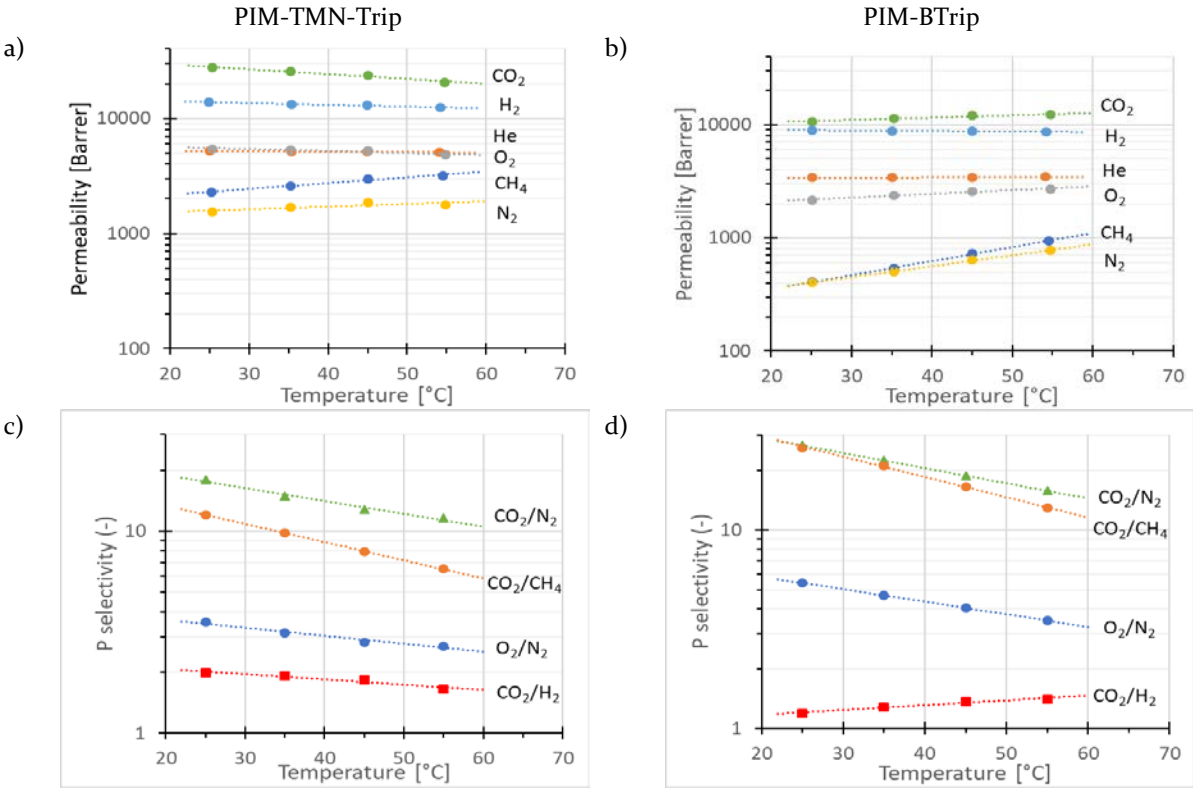

Figure 3. (a,b)Permeability coefficient and (c,d) ideal permselectivity of four relevant gas pairs for the thermally treated 100 days aged PIM-TMN-Trip and the 250 days aged PIM-BTrip as function of temperature. Dotted lines are least squares fit of the experimental data with an exponential equation. Numerical data are reported in Tables SI 1 and SI 2

For PIM-BTrip there is an increase in permeability with temperature for all the tested gases (Figure 3b) with the exception of the very small penetrants (H_2 and He), which remains almost constant. With rising temperature the selectivity for all the gas pairs decreases and its effect is strongest for CO_2/CH_4 (Figure 3c,d). The only exception is the gas pair CO_2/H_2 in PIM-BTrip (Figure 3d). For this range of temperatures in which both PIMs are physically and chemically stable, the temperature increase leads simultaneously to an improvement in the diffusivity coefficient and a reduction in solubility, and the net effect on the permeability coefficient depends on the most affected between solubility and diffusion.

The trends in *P* are better understood when looking at *D* and *S* individually. The diffusion coefficients of all gases increase with temperature (Figure 4a,b). The main effect of raising the temperature is an increased molecular vibration that facilitates the opening of a motion-enabled zone through which the penetrant gas can diffuse, in agreement with the theory of the non-specific activated diffusion process.[24] For the same reason, a lower diffusion coefficient is accompanied by a higher temperature dependence. The diffusion coefficients of H_2 and He are similar in both PIMs, whereas bulkier gases showed a markedly lower diffusion coefficient in PIM-BTrip. The enhanced diffusivity selectivity observed in PIM-BTrip clearly suggests a higher size-sieving behavior for this polymer with respect to PIM-TMN-Trip (Figure 4b).

Both polymers have nearly identical and extremely high gas solubility (Figure SI 3), for example, almost 100 times higher for CO_2 than in Pebax®1657 at 25°C.[25] To a large extent, their high permeability coefficients are due to extremely high gas solubility. In both PIMs, the gas solubility decreases with increasing temperature in a similar fashion, which is also reflected in the solubility selectivity. The latter decreases with increasing temperature (Figure SI 3 c,d) because the most soluble gases are usually more affected by a temperature change.

An overall analysis of the permeability, diffusivity and solubility coefficients reveals that diffusion is most affected by temperature in PIM-BTrip, resulting in an increasing permeability with temperature. In PIM-TMN-Trip, the relative contributions effect of temperature on the diffusion coefficients and on the solubility has different weights depending on the penetrant, causing different trends for all penetrants.

Entropic and energetic selectivity analysis

The temperature dependence of gas transport through a polymer membrane can be described by the Arrhenius-van't Hoff relationship:

$$P = P_0 \exp\left(\frac{-E_p}{RT}\right) \qquad \text{Eq. 3}$$

$$D = D_0 \exp\left(\frac{-E_d}{RT}\right) \qquad \text{Eq. 4}$$

$$S = S_0 \exp\left(\frac{-H_s}{RT}\right) \qquad \text{Eq. 5}$$

where, P_o, D_o, and S_o are temperature independent pre-exponential factors, R is the universal gas constant, T is absolute temperature, E_p and E_d are the activation energy of the permeation and diffusion respectively, and H_s is the heat of sorption. The activation energy of permeation and diffusion, as well as the heat of sorption is calculated from the experimental data using Eq. 3, Eq. 4, and Eq. 5, and listed in Table 1, while the pre-exponential factors are reported in Table SI 3.

The value for the activation energy of permeability (E_p) in PIM-BTrip is positive for all the gases with exception of H_2, while for PIM-TMN-Trip, E_p is positive for the bulky gases (N_2 < CH_4) and negative for the other four (He > H_2 > O_2 > CO_2). The negative value means that permeability decreases with temperature. This is unusual for traditional polymers used in gas separation. For example, PIM-1 shows positive values of E_p.[21] However, negative values for E_p have been reported for the transport of all gases through the ultrapermeable PTMSP.[22] All heats of sorption (H_s) are negative values, similar to those of PTMSP for H_2 and He, more similar to PIM-1 for N_2, O_2 and CH_4 and more negative for CO_2.[21] The value of H_s represents the strength of the polymer-sorbent interaction, which decreases when thermal motion increases. The activation energy of diffusion (E_d) for H_2 and He in PIM-TMN-Trip and PIM-BTrip are among the smallest values known, similar to those in PTMSP and smaller compared to those in PIM-1. These small values indicate a low energy barrier for diffusion, which is weakly influenced by the temperature. This can be ascribed to the presence of highly interconnected free volume (i.e. intrinsic microporosity).[21,22] In contrast, the E_d for O_2, CO_2, N_2 and CH_4 of the two very high permeable PIMs are similar to those found for PIM-1 (Figure 5), and much bigger than those in PTMSP. The slope of the activation energy of diffusion as a function of the square effective diameter follows the trend PIM-1 < PIM-TMN-Trip < PIM-BTrip (Figure 5). The steeper the slope, the higher the size-sieving behavior of the polymer. PTMSP has a very gentle slope in agreement with its very low diffusion selectivity. According to the transition theory of diffusion, the diffusion selectivity can be expressed as the product between entropic and energetic selectivity (Eq 6):[11]

$$\frac{D_x}{D_y} = \frac{\lambda_x^2}{\lambda_y^2} \underbrace{\exp\left(\frac{\Delta S^*_{d(x,y)}}{R}\right)}_{entropic\ selectivity} \underbrace{\exp\left(-\frac{\Delta E^*_{d(x,y)}}{RT}\right)}_{energetic\ selectivity} \qquad \text{Eq. 6}$$

where λ is the average diffusive jump which represent the distance between two neighboring cavities, R is the universal gas constant, T the absolute temperature, $\Delta S^*_{d(x,y)}$ the difference in the activation entropy of diffusion for two gases (x and y), and $\Delta E^*_{d(x,y)}$ is the difference in the activation energy of diffusion between the same gas pair. For a well packed medium, as in the case of the present dense membranes, the average diffusive jump length is proportional to the effective diameter of the penetrant gasthus even if the effective diffusive jump length is not known, the ratio λ_x^2/λ_y^2 can be approximated as d_x^2/d_y^2, where d is the effective diameter of the gases x and y.[10,26] In this work, the effective diameters estimated by Teplyakov and Meares are used for the approximation of the jump length, since these give the best correlation with D.[27] The energetic selectivity refers to the difference of energy needed to open a motion-enabled zone for diffusion for a gas over that required for N_2. Table 2 shows that for PIM-1, PIM-TMN-Trip and PIM-BTrip these values are all greater than one, except for CH_4. This is due to the bigger effective diameter of CH_4 compared with N_2, requiring a more extended motion-enabled zone for diffusion. The energetic selectivity of PTMSP is about 1, indicating that its free volume elements are interconnected by windows that are larger than the kinetic diameter of these gases. The energetic selectivity for O_2/N_2 separation in the three analyzed PIMs is within the range of high performing glassy polymers such as the 6FDA-TAB and 6FDA-TADPO (Figure 6)[12], but at much higher overall diffusion and permeability, resulting in similar energetic selectivity but at much higher permeability.

Table 1. Activation energies for Permeation (E_p) and diffusion (E_d), and heat of sorption (H_s), for six gases in PTMSP, PIM-1, PIM-TMN-Trip and PIM-BTrip

		Polymer			
Energy, kcal mol^{-1}	Gas	PTMSP[a]	PIM-1[b]	PIM-TMN-Trip[c]	PIM-BTrip[c]
E_p[d]	N_2	-1.2	2.8	1.06	4.34
	O_2	-1.6	0.6	-0.76	1.49
	CO_2	-2.3	0.4	-1.84	0.90
	CH_4	-1.5	4.2	2.27	5.55
	H_2	-0.6	0.4	-0.67	-0.21
	He	-0.1	0.6	-0.15	0.12
H_s[e]	N_2	-2.4	-3.1	-3.44	-3.11
	O_2	-2.8	-4.7	-3.38	-3.41
	CO_2	-2.4	-3.8	-4.85	-4.50
	CH_4	-2.7	-3.7	-3.12	-3.24
	H_2	-1.2	-2.8	-1.67	-0.77
	He	-1	-2.4	-1.53	-1.14
E_d[f]	N_2	1.2	6	4.50	7.45
	O_2	1.2	5.3	2.62	4.90
	CO_2	0.1	4.2	3.01	5.40
	CH_4	1.1	7.8	5.39	8.78
	H_2	0.6	3.2	1.00	0.57
	He	1	3	1.38	1.26

a) data from reference[22]; b) data from reference[21]; c) this work; d) Calculated from equation Eq. 3; e) Calculated from equation Eq. 4; f) Calculated from equation Eq. 5

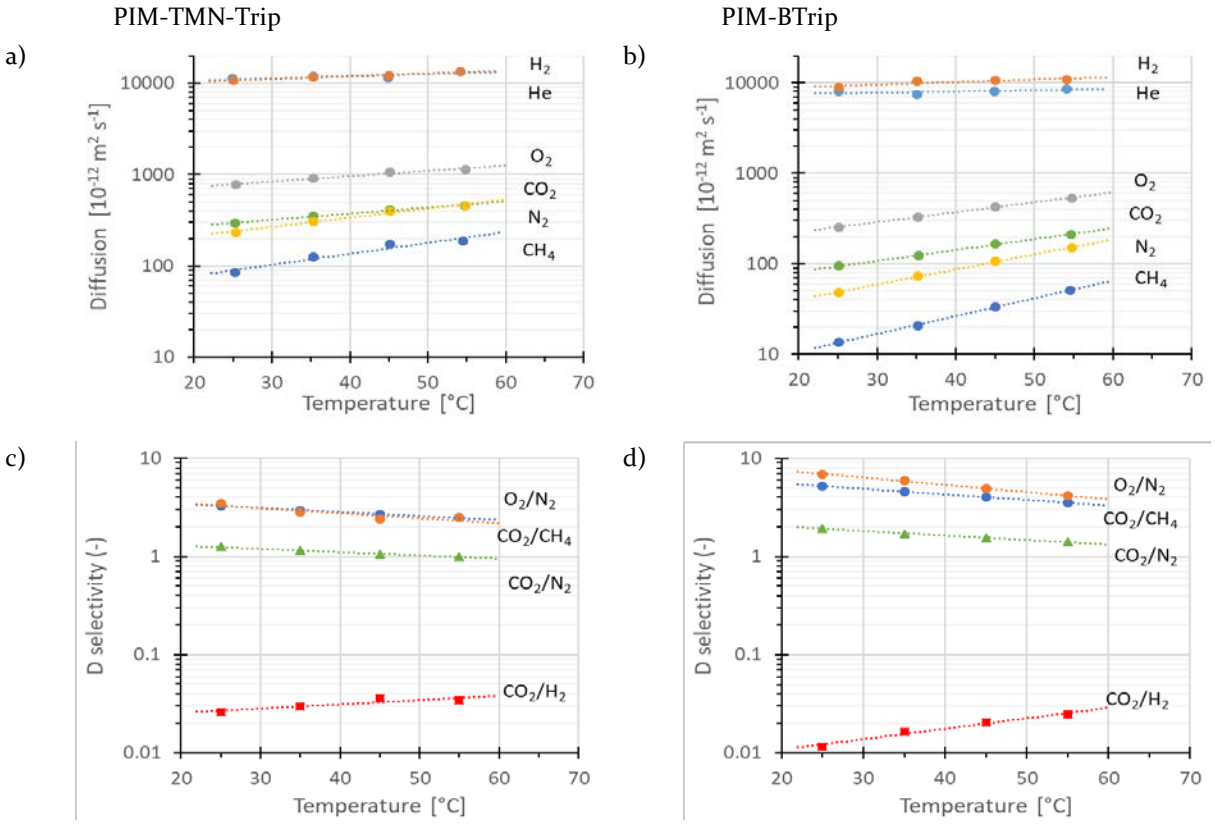

Figure 4. (a,b) Diffusion coefficient and (c,d) diffusion selectivity of four relevant gas pairs for the thermally treated 100 day aged PIM-TMN-Trip and the 250 day aged PIM-BTrip as function of temperature. Dotted lines are least squares fit of the experimental data with an exponential equation. Numerical data are reported in Tables SI 1 and SI 2-

He and H_2 have very high energetic selectivity in PIMs since the diffusion of these two small gases requires a smaller motion-enabled zone between molecular chains than the bulkier N_2, which needs more energy to open a gap between the very rigid polymer chains (Table 2). Further confirmation of the higher energetic selectivity of the PIM-BTrip membrane comes from the N_2 adsorption on powders at 77K, and therefore under very different conditions than those used for gas permeability measurements. It is notable that the PIM-TMN-Trip adsorbs significantly more N2 than PIM-BTrip at higher relative pressures, giving a larger value of apparent total pore volume (0.87 vs. 0.63 ml g^{-1}) and resulting in greater hysteresis between N_2 adsorption and desorption (Figure SI 1). This can be attributed to much greater swelling of PIM-TMN-Trip as N_2 is adsorbed, which is likely due to a smaller degree of polymer cohesion relative to PIM-BTrip, resulting from the bulky TMN substituents reducing the strength of intermacromolecular interaction between the naphthalene units protruding from the 2D polymer chains (Figure 1).

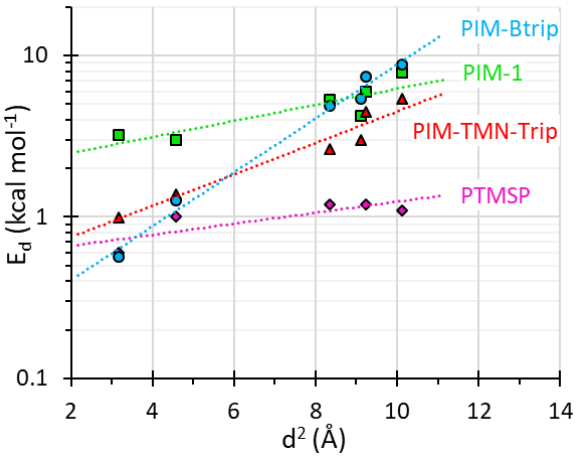

Figure 5. Activation energy of diffusion for PIM-1 (■)[21], PTMSP (◆)[22], PIM-TMN-Trip (▲) and PIM-BTrip (●) as a function of the gases effective diameter.[27] (Lines are plotted as a guide for the eyes)

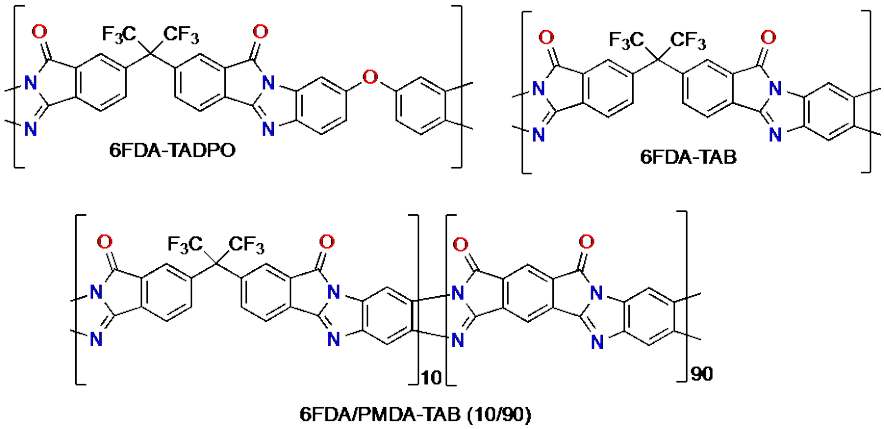

Figure 6 Molecular structures of 6FDA-TADPO, 6FDA-TAB, 6FDA/PMDA-TAB (10/90) discussed in reference [12]

Table 2. Diffusion selectivity (D_i/D_{N_2}) and correlated energetic and entropic selectivity for six gases at 25°C in the four polymers PTMSP, PIM-1, PIM-TMN-Trip and PIM-BTrip.

	Gas	PTMSP[a]	PIM-1[b]	PIM-TMN-Trip	PIM-BTrip
Diffusion	O_2	1.47	2.93	3.31	5.25
selectivity	CO_2	1.67	1.60	1.25	1.94
(i/N_2)	CH_4	1.07	0.33	0.36	0.28
	H_2	1.20	45.3	47.6 [d]	166 [d]
	He	0.73	44.0	45.7 [d]	184 [d]
Energetic[c]	O_2	1.00	3.26	24.1	74.1
selectivity	CO_2	6.41	20.9	12.5	31.9
(i/N_2)	CH_4	1.00	0.048	0.23	0.10
	H_2	2.75	113	371[d]	111773[d]
	He	1.40	159	194 [d]	34548 [d]
Entropic[c]	O_2	1.62	0.99	0.15	0.08
selectivity	CO_2	0.26	0.077	0.10	0.06
(i/N_2)	CH_4	0.97	6.37	1.48	2.44
	H_2	0.88	0.81	0.26 [d]	0.003 [d]
	He	1.52	0.81	0.69 [d]	0.016 [d]

a) diffusion selectivity data from reference [22]; b) diffusion selectivity data from reference [21]; c) the energetic and entropic selectivities are calculated this work; d) It should be noted that the calculated values for H_2 and He lose precision due to the fast membrane time-lag, which lead to a likely underestimation of the diffusion coefficient of max. 25%.

The lower polymer cohesion of PIM-TMN-Trip is consistent with its greater solubility in organic solvents and the lower energetic selectivity for diffusion. In contrast, the evidence of greater polymer cohesion of PIM-BTrip from N2 adsorption is likely to result in a film with a tighter pore structure, giving lower gas diffusion but higher selectivity than a film of PIM-TMN-Trip.

The entropic selectivity is related to the ability of a material to limit the degree of freedom of one gas molecule relative to another. Since the degree of freedom is associated with translational, rotational and vibrational modes of a molecule, the entropic contribution to diffusion is related to changes between a molecule in a normal state (when the molecule is within the micropores) and in a transition state (in a constricted window between micropores, i.e. a motion-enabled zone). Mathematically, the entropic contribution can be subdivided into 3 categories: high (>1) medium (≈1) and low (<1). Table 2 shows that the entropic selectivity for a gas over N_2 in PIMs is low for all gases with the exception of CH_4/N_2 for which it is greater than 1 in the investigated PIMs.

PIM-1 demonstrates O_2/N_2 entropic selectivity which is typical of that of semi-rigid polymers such as the previously investigated 6FDA-TAB and 6FDA-TADPO (Figure 6).[12] All three of these polymers are characterized by rigid fused-ring components linked together by flexible units (i.e. ether bonds, methylenes or spiro-centres).The inverse O_2/N_2 entropic selectivity of PIM-TMN-Trip and PIM-BTrip can be ascribed to the greater rotational mobility in the micropores of O_2 compared to N_2. Similar values were found for strongly diffusion selective polypyrrolone-based co-polymers, such as 6FDA-PMDA-TAB (10:90) (Figure 6), composed predominately of what was termed a "hyper-rigid" fused ring structure.[12] When the molecules have to diffuse through the windows between the micropores, the high rigidity of the triptycene-based polymers PIM-TMN-Trip and PIM-BTrip makes these windows similar to carbon molecular sieve pores, where O_2 and N_2 have similar entropy. Thus, the transition from a region where O_2 has a greater entropy than N_2, to a region where their entropy is similar, gives rise to reverse entropic selectivity. In the case of He/N_2 and H_2/N_2, this effect is even stronger, as highlighted by the very low entropic selectivity in the 250 days aged PIM-BTrip. These two light gases have more entropy in the free volume elements compared to bulkier gases. When they have to diffuse through a motion-enabled zone, their entropy is drastically reduced, and this reduction is relatively large with respect to the one experienced by bulky gases. This relative reduction leads to a large inverse entropic selectivity that is, nevertheless, swamped by a strong energetic selectivity that allow these polymers to exceed the proposed 2015 upper bound in the Robeson plots (Figure 2).

CONCLUSIONS

It can be concluded from this study that for triptycene-based PIMs, such as PIM-TMN-Trip and PIM-BTrip, the enhanced gas separation performances for O_2/N_2, H_2/N_2 and He/N_2 relative to those of PIM-1 and PTMSP are driven by strong energetic selectivity, with extremely high values demonstrated for PIM-BTrip. Hence, when the penetrant gas diffuses through the permanent microporosity of PIM-TMN-Trip and PIM-BTrip, the diffusion process is similar to that in molecular sieves, resulting in high diffusion coefficients. However, when the penetrant gas diffuses though a well-packed region of the polymer, the opening of a motion-enabled zone in PIM-TMN-Trip and PIM-BTrip requires a displacement of the very rigid polymer chains, which leads to high energetic selectivity as a function of the penetrant dimensions. The comparison with PIM-1 and PTMSP, highlights that the very rigid molecular structure of PIM-TMN-Trip and, especially, of PIM-BTrip, which does not possess the flexible TMN solubilizing group, enhances the energetic selectivity and thus the diffusion selectivity. This explains why the permselectivity properties of the aged PIM-BTrip exceeds the 2015 upper bounds for the O_2/N_2 and H_2/CH_4 gas pairs, which are particularly sensitive to diffusion selectivity. It should be noted that the permeability values obtained for this study are from thick films (>150 μm) aged for less than one year. Thinner films or those aged for longer are likely to demonstrate even higher selectivity.[28] In addition, the observed strong temperature dependence on selectivity noted during this study, originating from the enhanced energetic selectivity, means that operating membranes derived from these triptycene-based PIMs at lower temperatures may help to achieve commercially acceptable separation factors for several gas pairs. This is especially valid for the gas pairs CO_2/N_2 and CO_2/CH_4 were the enhanced by selectivity is accompanied by the enhanced permeability of CO_2 due its strong increase in solubility.

AUTHOR INFORMATION

Corresponding Author

* A. Fuoco E-mail: a.fuoco@itm.cnr.it / a.fuoco@europe.com
* N.B. McKeown E-mail: Neil.McKeown@ed.ac.uk

Present Addresses

‖ School of Chemistry, Cardiff University, Cardiff, UK.

Author Contributions

The manuscript was written through contributions of all authors. All authors have given approval to the final version of the manuscript.

Funding Sources

The work leading to these results has received funding from the European Union's Seventh Framework Program (FP7/2007-2013) under grant agreements n° 608490, project M4CO2.

REFERENCES

(1) Galizia, M.; Chi, W. S.; Smith, Z. P.; Merkel, T. C.; Baker, R. W.; Freeman, B. D. 50th Anniversary Perspective: Polymers and Mixed Matrix Membranes for Gas and Vapor Separation: A Review and Prospective Opportunities. *Macromolecules* **2017**, *50* (20), 7809–7843.

(2) Yampolskii, Y. Polymeric Gas Separation Membranes. *Macromolecules* **2012**, *45* (8), 3298–3311.

(3) Robeson, L. M. Correlation of Separation Factor versus Permeability for Polymeric Membranes. *J. Memb. Sci.* **1991**, *62* (2), 165–185.

(4) Robeson, L. M. The Upper Bound Revisited. *J. Memb. Sci.* **2008**, *320* (1), 390–400.

(5) Freeman, B. D. Basis of Permeability/Selectivity Tradeoff Relations in Polymeric Gas Separation Membranes. *Macromolecules* **1999**, *32* (2), 375–380.

(6) Budd, P. M.; Ghanem, B. S.; Makhseed, S.; McKeown, N. B.; Msayib, K. J.; Tattershall, C. E. Polymers of Intrinsic Microporosity (PIMs): Robust, Solution-Processable, Organic Nanoporous Materials. *Chem. Commun. (Camb).* **2004**, *10* (2), 230–231.

(7) Budd, P. M.; Elabas, E. S.; Ghanem, B. S.; Makhseed, S.; McKeown, N. B.; Msayib, K. J.; Tattershall, C. E.; Wang, D. Solution-Processed, Organophilic Membrane Derived from a Polymer of Intrinsic Microporosity. *Adv. Mater.* **2004**, *16* (5), 456–459.

(8) Yin, Y.; Guiver, M. D. Ultrapermeable Membranes. *Nat. Mater.* **2017**, *16*, 880.

(9) Rose, I.; Bezzu, C. G.; Carta, M.; Comesaña-Gándara, B.; Lasseuguette, E.; Ferrari, M. C. C.; Bernardo, P.; Clarizia, G.; Fuoco, A.; Jansen, J. C.; Hart, K.; Liyana-Arachchi, T. P.; Colina, C.; McKeown, N. B. Polymer Ultrapermeability from the Inefficient Packing of 2D Chains. *Nat. Mater.* **2017**, *16* (9), 932–937.

(10) Singh-Ghosal, A.; Koros, W. J. Energetic and Entropic Contributions to Mobility Selectivity in Glassy Polymers for Gas Separation Membranes. *Ind. Eng. Chem. Res.* **1999**, *38* (10), 3647–3654.

(11) Koros, W. J.; Zhang, C. Materials for Next-Generation Molecularly Selective Synthetic Membranes. *Nat. Mater.* **2017**, *16*, 289.

(12) Zimmerman, C. M.; Koros, W. J. Entropic Selectivity Analysis of a Series of Polypyrrolones for Gas Separation Membranes. *Macromolecules* **1999**, *32* (10), 3341–3346.

(13) Singh, A.; Koros, W. J. Significance of Entropic Selectivity for Advanced Gas Separation Membranes. *Ind. Eng. Chem. Res.* **1996**, *35* (4), 1231–1234.

(14) Ma, Y.; Zhang, F.; Yang, S.; Lively, R. P. Evidence for Entropic Diffusion Selection of Xylene Isomers in Carbon Molecular Sieve Membranes. *J. Memb. Sci.* **2018**, *564*, 404–414.

(15) Bernardo, P.; Bazzarelli, F.; Tasselli, F.; Clarizia, G.; Mason, C. R.; Maynard-Atem, L.; Budd, P. M.; Lanč, M.; Pilnáček, K.; Vopička, O.; Friess, K.; Fritch, D.; Yampolskii, Y. P.; Shantarovich, V.; Jansen, J. C Effect of Physical Aging on the Gas Transport and Sorption in PIM-1 Membranes. *Polymer (Guildf).* **2017**, *113*, 283–294.

(16) Ma, X.; Pinnau, I. Effect of Film Thickness and Physical Aging on "Intrinsic" Gas Permeation Properties of Microporous Ethanoanthracene-Based Polyimides. *Macromolecules* **2018**, *51* (3), 1069–1076.

(17) Fraga, S. C.; Monteleone, M.; Lanč, M.; Esposito, E.; Fuoco, A.; Giorno, L.; Pilnáček, K.; Friess, K.; Carta, M.; McKeown, N. B.; Izak, P.; Zetrupovà, Z.; Crespo, J. G.; Brazinha, C.; Jansen, J. C. A Novel Time Lag Method for the Analysis of Mixed Gas Diffusion in Polymeric Membranes by On-Line Mass Spectrometry: Method Development and Validation. *J. Memb. Sci.* **2018**, *561*, 39–58.

(18) Swaidan, R.; Ghanem, B.; Pinnau, I. Fine-Tuned Intrinsically Ultramicroporous Polymers Redefine the Permeability/Selectivity Upper Bounds of Membrane-Based Air and Hydrogen Separations. *ACS Macro Lett.* **2015**, *4* (9), 947–951.

(19) Carta, M.; Croad, M.; Malpass-Evans, R.; Jansen, J. C.; Bernardo, P.; Clarizia, G.; Friess, K.; Lanč, M.; McKeown, N. B. Triptycene Induced Enhancement of Membrane Gas Selectivity for Microporous Tröger's Base Polymers. *Adv. Mater.* **2014**, *26* (21), 3526–3531.

(20) S., G. B.; Raja, S.; Eric, L.; Ingo, P. Ultra-Microporous Triptycene-Based Polyimide Membranes for High-Performance Gas Separation. *Adv. Mater.* **2014**, *26* (22), 3688–3692.

(21) Li, P.; Chung, T. S.; Paul, D. R. Temperature Dependence of Gas Sorption and Permeation in PIM-1. *J. Memb. Sci.* **2014**, *450*, 380–388.

(22) Masuda, T.; Iguchi, Y.; Tang, B.-Z.; Higashimura, T. Diffusion and Solution of Gases in Substituted Polyacetylene Membranes. *Polymer (Guildf).* **1988**, *29* (11), 2041–2049.

(23) Rose, I.; Carta, M.; Malpass-Evans, R.; Ferrari, M.-C.; Bernardo, P.; Clarizia, G.; Jansen, J. C.; McKeown, N. B. Highly Permeable Benzotriptycene-Based Polymer of Intrinsic Microporosity. *ACS Macro Lett.* **2015**, *4* (9), 912–915.

(24) BARRER, R. M. Nature of the Diffusion Process in Rubber. *Nature* **1937**, *140*, 106.

(25) Bernardo, P.; Jansen, J. C.; Bazzarelli, F.; Tasselli, F.; Fuoco, A.; Friess, K.; Izák, P.; Jarmarová, V.; Kačírková, M.; Clarizia, G. Gas Transport Properties of PEBAX®/Room Temperature Ionic Liquid Gel Membranes. *Sep. Purif. Technol.* **2012**, *97* (ILSEPT2011 Special Issue), 73–82.

(26) Crank, J. *The Mathematics of Diffusion*, 2nd ed.; Clarendon Press: Oxford, 1975.

(27) Teplyakov, V.; Meares, P. Correlation Aspects of the Selective Gas Permeabilities of Polymeric Materials and Membranes. *Gas Sep. Purif.* **1990**, *4* (2), 66–74.

(28) Bezzu, C. G.; Carta, M.; Ferrari, M.-C.; Jansen, J. C.; Monteleone, M.; Esposito, E.; Fuoco, A.; Hart, K.; Liyana-Arachchi, T. P.; Colina, C.; McKeown, N. B. The Synthesis, Chain-Packing Simulation and Long-Term Gas Permeability of Highly Selective Spirobifluorene-Based Polymers of Intrinsic Microporosity. *J. Mater. Chem. A* **2018**, *6* (22), 10507–10514.

Graphical Abstract